# Journal of Applied Sciences

ISSN 1812-5654

science alert

ANSInet
an open access publisher
http://ansinet.com

Journal of Applied Sciences 5 (3): 517-526, 2005
ISSN 1812-5654


# Nanosecond Laser Flash Photolysis: Dealing with Dynamic-range and Response-time Limitations of the Detection System

Valentine I. Vullev and Guilford Jones, II
Photonics Center, Boston University, 8 St. Mary's St., Boston, MA 02215, USA

**Abstract:** Nanosecond laser flash photolysis (LFP) is an indispensable technique for photoinduced kinetic studies either by transient absorption or time-resolved emission measurements. Despite the commercialization of the instruments that can be used for conducting this type of measurements, many researcher still prefer to assemble their own LFP apparatuses in order to adjust them to the nature of their work and allow optimization and expandability. In this article we described in detail the nanosecond LFP apparatus that has been assembled and used in our laboratory. Significant limitations on this technique are imposed by its sensitivity and the time range that it can cover. These issues have been addressed by a design of a detector assembly that takes advantage of a fast head-on photo-multiplier tube, which is powered through an active bleeder circuit designed after detector circuitry used in high-energy physics experiments. In addition, a high-precision compensating circuit is employed to remove the DC component of the signal. High sensitivity and a working time range from tens of nanoseconds to tens of seconds (or longer) were achieved without compromising the speed of the detection required for nanosecond transient absorption. The described detector and the whole LFP apparatus have considerably simpler control interface in comparison to other instruments of this type. The work of the apparatus is illustrated with examples of transient absorption and time-resolved emission data for solutions of ethyl eosin and terbium (III) dipicolinate complex, respectively.

**Key words:** Nanosecond LFP, dynamic range, detection system

## INTRODUCTION

This paper presents a technical description of a nanosecond laser flash photolysis (LFP) apparatus that was built in our laboratory and for several years, has been successfully used for collecting transient absorption[1,2] and time-resolved emission data[3,4]. Herein, we concentrate on the design and performance of the detection system of the LFP apparatus.

Transient absorption spectroscopy is an indispensable tool in investigations of fast kinetics[5,6]. In nanosecond LFP, the change in the optical density (ΔOD) of a sample upon photoexcitation is monitored using a CW probe light. The data are collected either as a sequence of transient spectra at successive times after the excitation pulse, or as separate decay curves at each of the wavelengths in the spectral range of interest. In both cases, a matrix that represents ΔOD as a function of time and wavelength is produced.

In nanosecond transient absorption experiments, quantitative recording of fast and weak signals on a continuous, DC, background is required. Because the background can be as much as four orders of magnitude more intense than the signal of interest, there is a significant demand on the sensitivity and the dynamic range of the photodetectors. For nanosecond LFP systems that record the data as series of decays at fixed sequential wavelengths, the preferred detection methods involve photo-multiplier tube (PMT) assemblies. Despite their high sensitivity and wide linear-response dynamic range spanning 4-7 orders of magnitude, the side-on PMTs, which are used most frequently, manifest relatively long response times. An improvement of the working rates is usually achieved by short-circuiting the last few dynode stages with the anode[7]. This approach, however, compromises significantly PMT sensitivity. Therefore, to compensate for relatively low detector sensitivity, frequently the intensity of the probe-light is increased 10-100 fold during data acquisition by applying a voltage strobe, longer than the duration of the measurement, to the probe lamp power supply immediately before the laser excitation pulse[7-9]. In addition to decreasing the response times, short-circuiting the last few dynode stages of the PMT and pulsing the probe light source result in larger

**Corresponding Author:** Dr. Valentine I. Vullev, Department of Chemistry and Chemical Biology, Harvard University, 12 Oxford Street, Cambridge, MA 02138, USA Tel: 617 9436 Fax: 617 495 2500
E-mail: vullev@fas.harvard.edu

cathode photocurrents leading to smaller signal-to-noise ratios[10]. Although this approach has proven its usefulness, it has some serious disadvantages, such as: 1. A limitation on the length of the acquisition time is imposed by a baseline drift that occurs in the late microsecond and/or millisecond domain depending on the capacitance of the bank that provides the voltage boost; 2. The large intensity of the probe-light can result in sample photodegradation and/or increased emission; and 3. The voltage throb causes a high stress on the arc lamp used, leading to significant shortening of its lifetime.

The nanosecond LFP apparatus described here uses 8-ns laser pulses at 266, 355 and 410-710 nm for an excitation source. Transient absorption or emission data are collected as a series of decays at sequential wavelengths by using a PMT assembly. Our efforts were concentrated on the development of a fast-response detector module that can collect high quality data without applying a voltage strobe to the power supply of the probe light. The improved design of the detector was achieved by the employment of: (i) a fast head-on PMT[11]; (ii) an active bleeding circuit[10,12], increasing the PMT dynamic range more than an order of magnitude and (iii) a compensating circuit[6,13-15], providing analogue subtraction of the intense DC component of the acquired data, which improves the detection of weak AC signals. Data is presented that demonstrate the stability and sensitivity of the system. Using fast components in this design assures subnanosecond rise time of the detector. As a result, the limitation on the fastest rates measured is imposed by the excitation pulsewidth.

## MATERIALS AND METHODS

**Instrument setup:** A Nd-YAG laser (Surelite II-10, Continuum) equipped with double, triple and quadruple harmonic generators, is employed as a source of 8 ns excitation pulses at 532, 355 and 266 nm. In addition, a tunable optical parametric oscillator (OPO) provides excitation in the wavelength region between 410 and 710 nm. The laser pulse is delivered to the sample cell at 90° to the CW probe light, covering the whole cell width.

The probe light from a 75 W xenon arc lamp (horizontal housing, PTI) is controlled by a probe-light shutter placed in front of the lamp housing. The beam is collimated before passing only through the cell volume that is illuminated by the laser and then focused on the slit of a double-grid monochromator (DH-10, Instrument SA; blaze wavelength 450 nm, linear dispersion-1200 gratings/mm, selectable slit widths 0.5, 1 and 2 nm), to which the detection module is attached. An air-cooled IR filter is placed immediately after the arc lamp in order to prevent overheating and subsequent damage to the probe-light optics. Cutoff optical filters are placed before the sample to suppress any emission due to excitation by the short-wavelength probe light. Identical filters are installed in front of the monochromator to suppress $k\lambda_{ex}$ (where k = 2, 3,…) detection of scattered light from the excitation laser pulse. From the detection module, the signal is forwarded to a digital oscilloscope (LeCroy 9361). Control of the apparatus and the recording of data are performed with LabView (version 5.0, National Instruments), which is run on a Windows NT 4.0 workstation. The system interface with the CPU is realized through two serial ports (RS-232 connections) and two PCI boards (GPIB and MIO-16E-4, both from National Instruments). Data acquisition is triggered by a signal either from a fast photodiode assembly, or from the variable-sync-out of the laser, depending of the time domain of the measurement.

**Detector assembly:** Signal detection is performed by a fast Metal Package head-on PMT (R5600U-04, Hamamatsu) that is powered through an active bleeder circuit with an adjustable voltage divider and an independent high voltage (HV) supply for the cathode (Fig. 1a). A transistor-based PMT active bleeder circuit, first developed for high-energy physics experiments[12], is considerably more advantageous for this application than the alternative Zener-diode active circuit[10], because the former allows alteration of the dynode potentials through the adjustable voltage divider offering an easy way to set the optimal working conditions for the PMT. The capacitors at the base of the PMT are selected to cover the time range from picoseconds to hundreds of nanoseconds: 0.1 nF, 1 nF, 10 nF, 0.1 μF, 1 μF and 47 μF for $C_{1, 2, 3, 4, 5 \text{ and } 6}$, respectively. During that time interval, the high-voltage transistors, T (MPSA42, Fairchild Semiconductors, $f_T$ = 50 MHz), will react and deviate the necessary amount of current from the voltage divider to the PMT, maintaining a constant potential at each dynode[12].

The CW probe light produces a strong DC component that is removed from the measured signal by a compensating circuit designed to carry fast signals. The design of this circuit is based on a DC precision amplifier with automatic null offset[13]. In order to prevent nanosecond-signal distortion, only a single fast operational amplifier was used with feedback parameters that provide the optimal bandwidth (Fig. 1b, 1c and 1d). The current from the PMT is terminated at $R_{pmt}$ (250 Ω) and the ensuing signal voltage, $V_s$, is forwarded to the non-inverting input terminal of a fast operational amplifier, $OA_1$ (LM7171, National Semiconductor), whose feedback is

referenced to $V_g$. The signal current produced from $OA_1$ is sent to an oscilloscope through a coaxial cable with an impedance of 50 Ω. In order to prevent ringing, a termination with matching impedance, $R_{tm}$ (50 Ω), is placed before the coaxial cable, matching the termination in the oscilloscope (50 Ω, DC coupling). In addition, detectable ringing between the PMT, $R_{pmt}$ and $OA_1$ is avoided by keeping those connections shorter than 5-10 mm. The interface between the compensating circuit and the CPU is realized through a quad bilateral switch (CD4066BC, Fairchild Semiconductor) (Fig. 1c). The four switches are controlled by two gate signals generated from a relay array (ER-8) controlled by the digital I/O terminals of the PCI-MIO-16E-4 interface board. The compensating circuit has two states achieved by the Zeroing and Grounding gates.

**Zero reference:** When a CW background signal is measured ($V_s = V_{cw}$) and the zeroing gate is on, a connection between points C and B is realized. Thus, the output voltage from $OA_1$, $V_{out}$, is fed into the inverting input terminal of $OA_2$, generating an amplified output, $V_m$, opposite in sign to $V_{out}$, which is set as the reference voltage, $V_g$, after an inversion through $OA_3$ (Fig. 1b). In order to match all the circuit values, the memory capacitor, $C_m$ (an assembly of five tantalum capacitors of 6.8 μF each, connected in parallel), is gradually charged with a voltage value of-$V_{cw}$, thus, making $V_{out} = V_s - V_g = V_{sw} - V_{sw} = 0$. The zeroing gate is kept on for one second during which time $C_m$ becomes completely charged (Fig. 2a). Thus, the reference voltage $V_g$ of $OA_1$ is set to the background voltage, $V_{cw}$, stored in $C_m$. In addition, $C_m$ is stabilized by a charge-leakage compensator connected to points A and B (Fig. 1d).

**Ground reference:** When the grounding gate is turned on (Fig. 1c), the switches A, B and D are closed, causing the two terminals of $C_m$ to be connected to the ground. Thus, the output voltage $V_m$ and consequently, the reference $V_g$ will acquire ground potential and as a result, the PMT signal will be referenced to the common ground of the apparatus. The grounding gate is kept on for about half a second allowing sufficient time for the complete discharge of $C_m$ (Fig. 2a).

**Acquisition sequence:** At each wavelength transient absorption data, when emission correction is required, are acquired in the following steps:

1. The probe-light shutter should be closed
2. Zeroing the compensating circuit
3. Firing the laser and recording the intensity of the emission signal, $\Delta I_E$
4. Opening the probe light shutter
5. Grounding the compensating circuit
6. Measuring the probe light intensity, $I_0$
7. Zeroing the compensating circuit
8. Firing the laser and recording the intensity of the signal, $\Delta I'$, that contains emission and transient absorption components
9. Closing the probe light shutter and grounding the compensating circuit
10. Signal correction, i.e., $\Delta I = \Delta I' - \Delta I_E$. In addition, $I_0$ is corrected for the dark signal, $I_d$, that is measured while the probe-light shutter is closed and the compensating circuit is grounded and is a result of the PMT dark current and/or offset in the circuit when $V_m$ is at ground potential. However, that correction can be omitted with no serious concern since the measured $I_d$ is in the vicinity of 4 mV, while the normal working range of $I_0$ is about-1 V.

When the emission correction is not needed, the steps 1, 2, 3 and 10 are omitted. For time-resolved emission and excitation pulse profile measurements, only steps 1, 2 and 3 are used.

Under the applied experimental conditions, the recorded voltage, $V_{out}$, is linearly proportional to the light intensity. The emission and pulse profile data (i.e., $\Delta I_E$ vs. time) are reported in negative volts, where the negative sign indicates that the photocurrent of emitted electrons has opposite direction to the positive charge flow. The values of transient absorption are obtained from ratio involving $\Delta I$ and $I_0$:

$$\Delta OD = 1g\left(\frac{I_0}{\Delta I + I_0}\right) \quad (1)$$

Ethyl eosin was purchased from Aldrich and recrystallized from ethanol. Dipicolinic acid and terbium trichloride were obtained from Aldrich and used as received. Phosphate buffer (50 mM, pH 7) was purchased from Fisher Scientific. In all experiments Milli-Q water was used and the samples were purged with argon immediately before the measurements.

## RESULTS AND DISCUSSION

### Design of the detector assembly

**PMT choice:** The choice for PMT was governed by the following requirements: (1) wide DC and pulse linearity ranges in order to handle signals in the background of an intensive CW light; (2) fast response time, characterized by the rise and fall times and by the transient time spread (TTS)[11]; (3) relatively high sensitivity, so that the

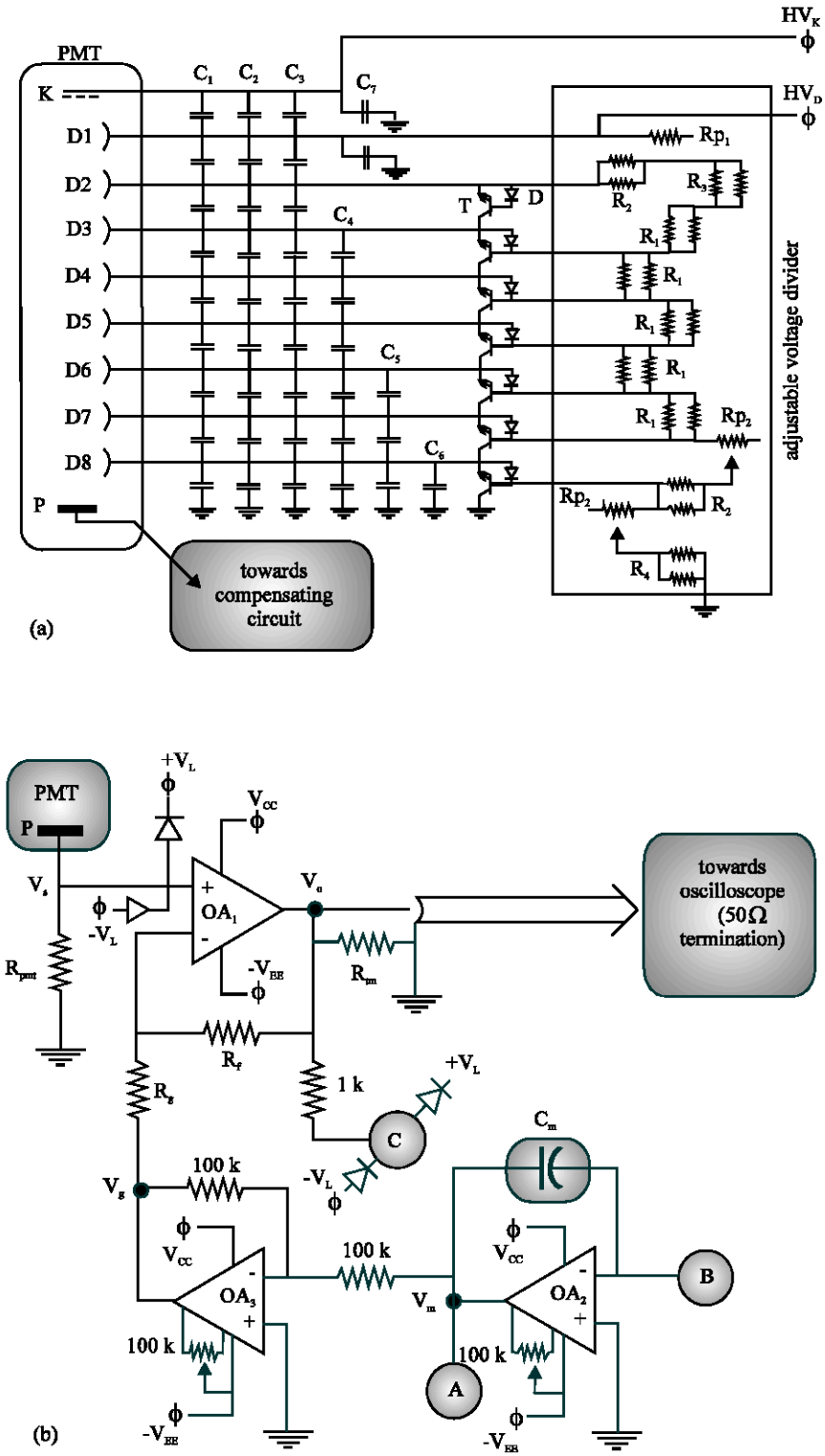


Fig. 1: Schematics for: (a) PMT bleeder circuit, (b) compensating circuit

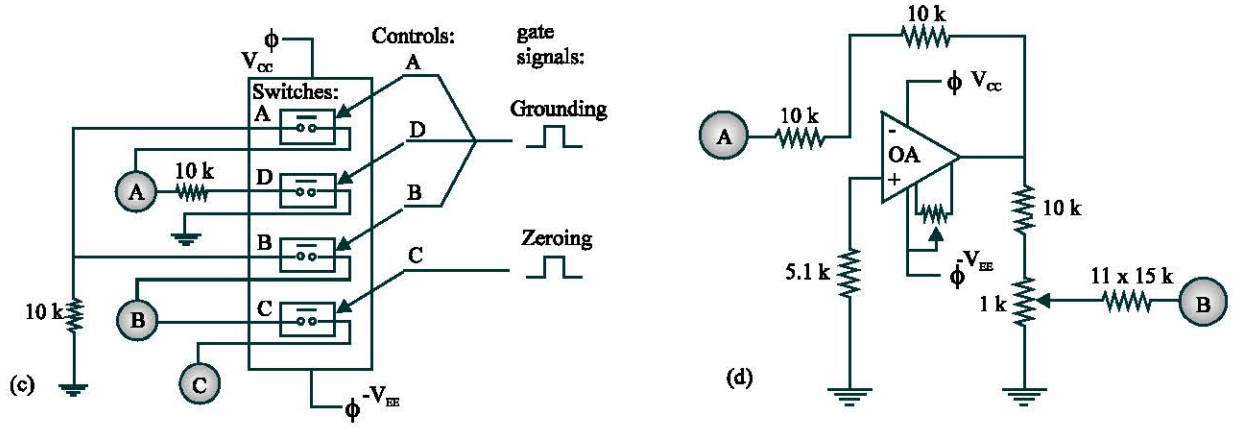


Fig. 1: Schematics for: (c) wiring of the quad bilateral switch, (d) charge-leakage compensator

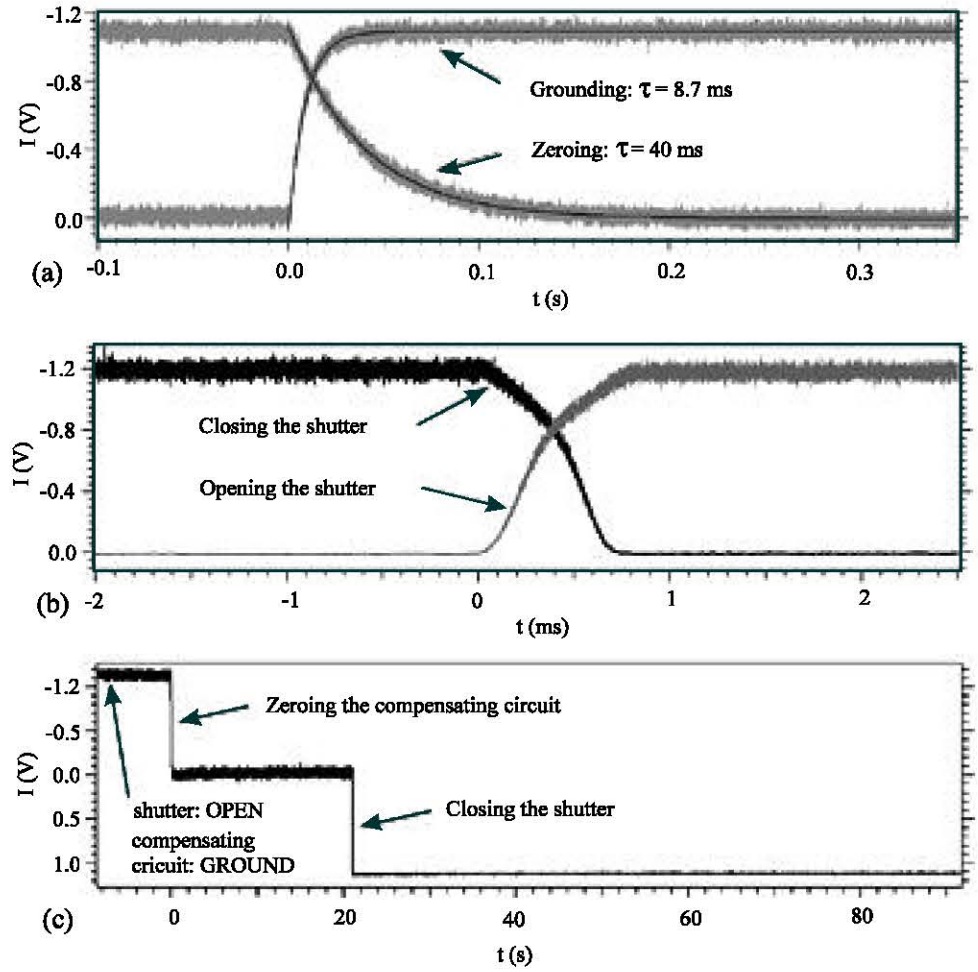


Fig. 2: Various tests of the response and stability of the compensating circuit: (a) zeroing and grounding with the corresponding time constants while the probe-light shutter is open, (b) closing and opening the probe-light shutter while the compensating circuit is in set to ground, (c) long-term stability of the compensating circuit

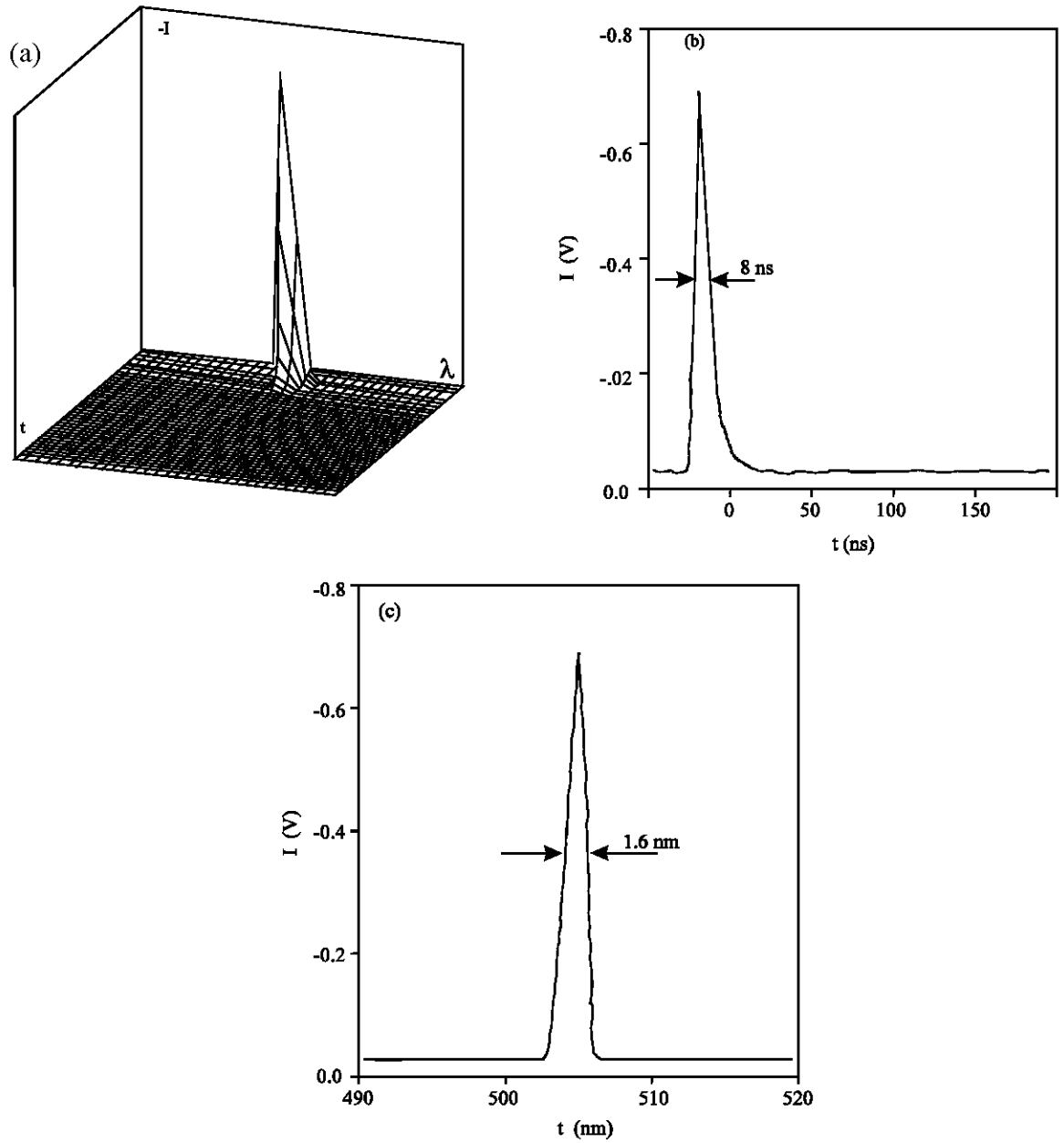


Fig. 3: Profile of an excitation laser pulse at 505 nm: (a) time and wavelength distribution of the relative intensity, -I, (b) dependence of intensity on time, (c) dependence of intensity on wavelength

detector can be used for measuring time resolved emission when the lifetimes are sufficiently long. The traditionally used side-on photomultipliers manifest wide DC linearity and sensitivity from the near IR to the UV spectrum, however, their time characteristics are not satisfactory enough: e.g., rise times in the order of 1-2 ns and TTS of about 3-10 ns. On the other hand, the microchannel plate (MCP) head-on PMTs have superior time characteristics (e.g., rise times of 150-180 ps and TTS of 25-90 ps) and pulse linearity of up to 350 mA of anode current. However, MCP PMTs are lacking sufficient DC linear range, therefore, they were not under consideration in our design.

Small metal package head-on PMTs with metal channel dynodes have been developed about a decade ago and they possess numerous characteristics needed for our application. The reported rise and fall times of these photomultipliers are 650 ps and 1.05 ns, respectively, manifesting TTS of 280 ps and gain of $3\times10^5$ under the same conditions[11]. Furthermore, the R5600

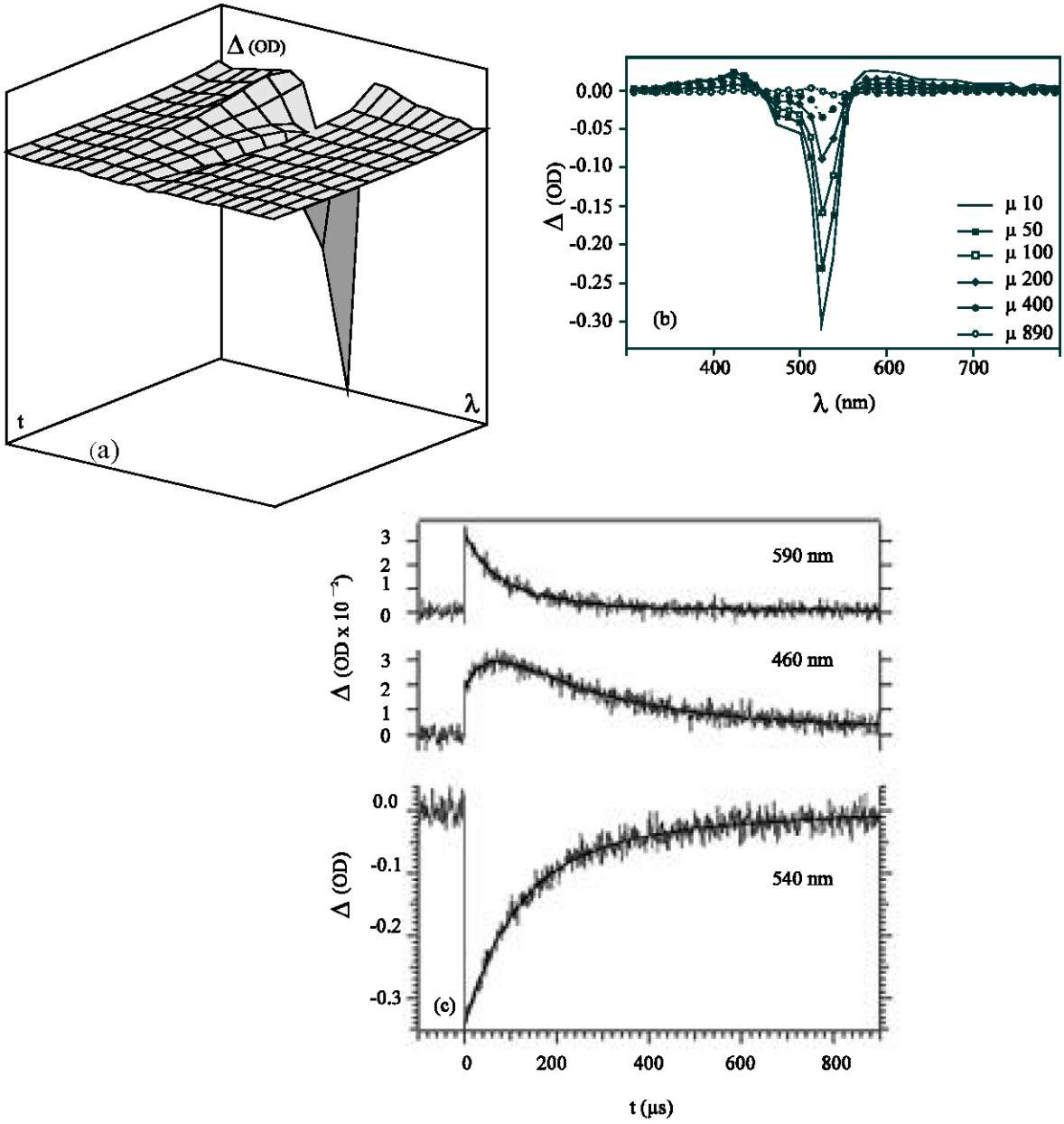


Fig. 4: Transient absorption spectra of ethyl eosin (16 μM in DMF; $\lambda_{ex}$ = 505 nm; 10 mJ/pulse): (a) time and wavelength distribution of the change in optical density, ΔOD, (b) transient absorption spectra recorded at different times after the excitation laser pulse, (c) decay curves recorded at different wavelengths

PMTs exhibit pulse linearity of up to 30 mA anode current and when powered through the active bleeder circuit on Fig. 1a, the measured DC linearity exceeded 3 mA, however, the data acquisition are usually run at $V_{out}$ ~-1 V, corresponding to anode current of 2 mA.

The signal-to-noise ratio, (S/N), limitations arising from the PMT can be estimated from the cathode, $i_k$, or anode, $i_p$, currents[16,17]:

$$S/N \approx \sqrt{\frac{i_k}{2e\Delta f}\frac{\delta-1}{\delta}} = \sqrt{\frac{i_p}{2e\mu F\Delta f}\frac{\delta-1}{\delta}} \quad (2)$$

where Δf is the frequency bandwidth of the measurement, e is the electron charge, F is the electron collection efficiency representing the probability of an accelerated electron to cause an avalanche upon striking the

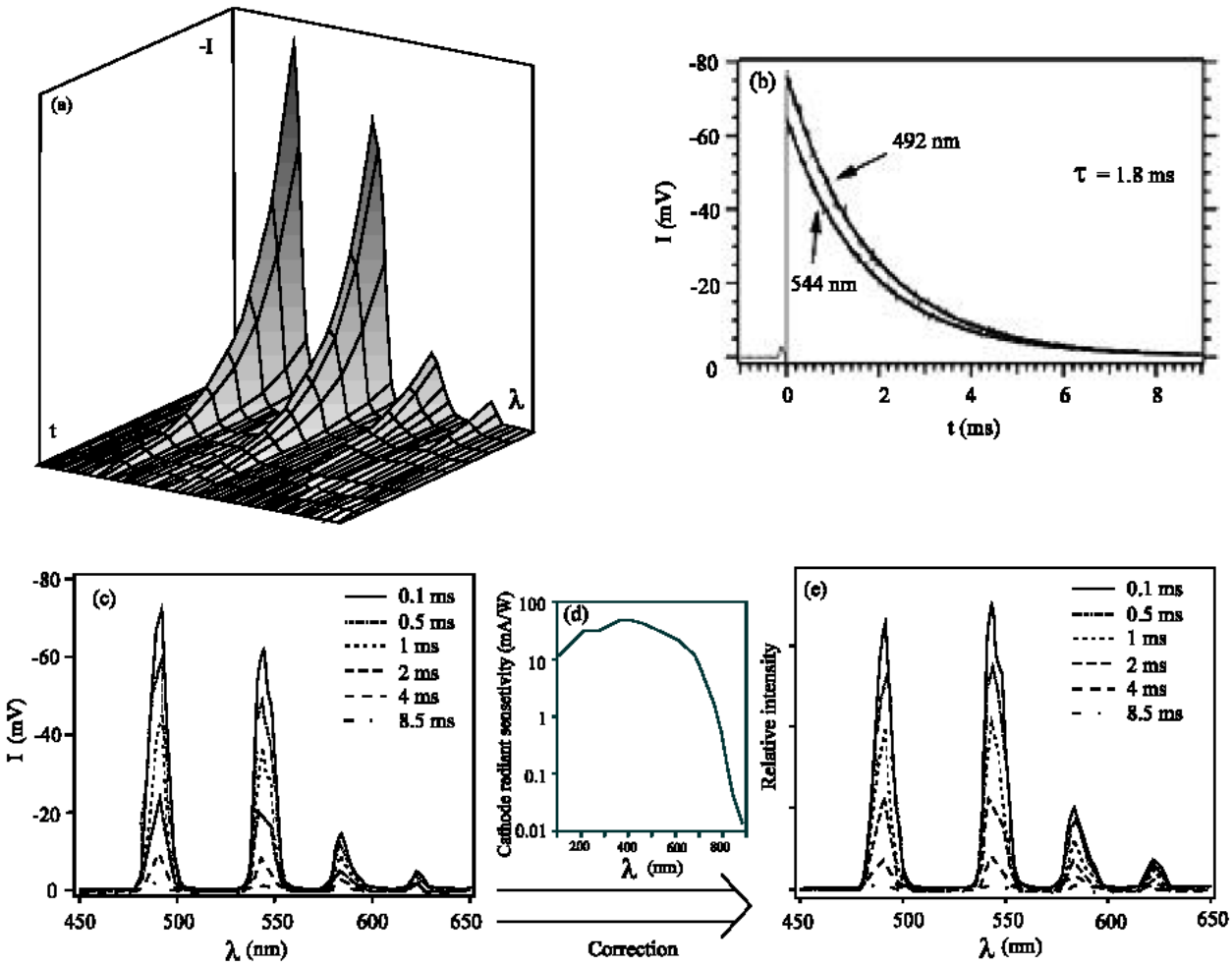


Fig. 5: Time resolved emission data for terbium (III) dipicolinate complex (17 μM $TbCl_3$ and 51 μM dipicolinic acid in water, pH 6; $\lambda_{ex}$ = 266 nm; 10 mJ/pulse): (a) time and wavelength distribution of the change in the emission intensity,-I, (b) emission decay curves recorded at different wavelengths, (c) uncorrected emission spectra recorded at different times, (d) correction for the sensitivity of the PMT, (e) the corresponding corrected emission spectra at different times

dynode[18], μ is the PMT gain and δ is the average gain at each stage, hence, for an n-stage photomultiplier, $\delta^n = \mu$.

Taking into consideration equation 1, the expression for S/N ratio can be applied to the PMT circuitry on Fig. 1:

$$S/N \approx \sqrt{\frac{t_{dp} \mid V_0(10^{-\Delta OD}-1) \mid}{2eA_{OA1}R_{pmt}F} \cdot \frac{\sqrt[n]{\mu}-1}{\sqrt[n]{\mu^{n+1}}}} \qquad (3)$$

where, $V_0$ is the measured voltage value of $I_0$, ΔOD is the measured transient absorption, $A_{OA1}$ is the closed-loop gain of $OA_1$ (Fig. 1b) and $t_{dp}$ is the time difference between two consecutive data points.

From equation 3 it can be estimated that when recording ΔOD of ~ 0.01 with time resolution of 1 ns the maximum signal-to-noise ration will be expected to be about 3.9 should ten measurements be averaged. When the time resolution is decreased to 10 ns per a data point, the same signal-to-noise can be achieved with solely a single measurement. In addition, at resolution of 1 μs per a point and ΔOD ~ 0.001, S/N of about 12 can be achieved with one measurement and the same quality of measurement will be expected for ΔOD ~ $10^{-4}$ should the time resolution is dropped to 10 μs per a data point.

**Compensating circuit:** Inputting the DC correction as a steady current through a T-type cable connection has been used in various designs[14,15,19], however, such an approach presents difficulties in impedance matching leading to signal ringing. This problem is addressed by

taking an advantage of a fast operational amplifier, $OA_1$ (Fig. 1b), which provides 50 Ω coupling with the oscilloscope through the termination at $R_{tm}$. The feedback of $OA_1$ is designed to provide the widest frequency bandwidth without a significant concern about the closed-loop gain. Since $OA_1$ and $R_{pmt}$ are right at the base of the PMT and the connections between these elements and the anode are kept only a few millimeter long, the signal amplification can be achieved by increasing the value of $R_{pmt}$, rather than by increasing the closed-loop gain of $OA_1$. (However, $R_{pmt}$ should not be allowed to exceed a kiloohm because that will lead to increase in the amplifier shot noise)[20]. Figure 2 shows DC signal recorded at open and closed probe-light shutter with the compensating circuit zeroed or grounded. Apparently, the noise increases significantly upon illumination of the PMT, while the charging and discharging of $C_m$ (i.e., zeroing and grounding of the circuit) practically does not influence the noise level, indicating that the photomultiplier, rather than the compensating circuit, is the principal contributor to the signal noise. Thus, the signal-to-noise limit can be reliably estimated by equation 3.

The stability of the compensating circuit is demonstrated on Fig. 2c. When $C_m$ is charged with about 1.2 V, the baseline drifts about 7 mV/s (~ 0.6 % / s) for the first two seconds after the zeroing gate is turned off and for the next 10-30 seconds, during which time the data are a cquired, the baseline drifts less than 0.5 mV/s (~0.04% / s).

**Examples of time-resolved data:** This particular LFP apparatus has been under extensive use in our laboratory and the quality of the measurements is demonstrated by selected examples for time / frequency (wavelength) data in three different time domains (Fig. 3-5). The laser pulse profile data (Fig. 3) are a result of an average of five measurements per wavelength acquisition, while the transient absorption and emission data are obtained by averaging only two measurements (Fig. 4 and 5). Although $\Delta OD(\lambda)$ is not dependent on the alterations in the PMT sensitivity with variations of the wavelength, the emission spectral data have to be corrected for the PMT response to radiant power (Fig. 5c, 5d and 5e).

The data on Fig. 4 show eosin triplet formation with the 8-nanosecond excitation pulse and consequent decay observed at 590 nm[21]. The bleach recovery at 540 nm and the formation and the decay of the reduced eosin moiety at 460 nm are evidence for intermolecular electron transfer between the excited chromophores[22]. On the other hand, Figure 5 depicts the monoexponential emission decay of terbium (III) dipicolinate, yielding a lifetime of 1.8 ms[3,23,24].

Since the principal noise source associated with this apparatus is the PMT, the signal-to-noise ratio of the measured data can be improved by increasing the cathode current (equation 2). In the side-on PMTs, such a current increase has been achieved through decreasing the total gain, μ, by short-circuiting the last few dynode stages with the anode, thus, preventing saturations at high $i_k$. Since R5600 photomultipliers are recently developed and to our knowledge, they have not been used in transient absorption applications, there are no reports on how the PMT performance will alter upon eliminating some of the later stages. Therefore, in order to improve the detector design in this manner, a thorough analysis of R5600 PMT, described by Fenster *et al.*[10], is required.

Detection time limitations of 1-3 ns are imposed by the operational amplifier $OA_1$ and the oscilloscope, which are longer than the PMT response time. However, the time limiting factor in the LFP measurements is the duration of the laser excitation pulse (Fig. 3). Therefore, any further improvement on the time characteristics of the detector is pointless unless shorter excitation pulses are applied.

In conclusion, a detector assembly is described that takes advantage of fast head-on PMT equipped with parallel metal plates of channeled dynodes. An active bleeder circuit increases the DC linearity without applying large currents to the voltage divider. A compensating circuit provides analogue subtraction of the DC component of the signal and is considerably simpler than other baseline correction devices previously described. In spite of its simplicity, the described circuit offers excellent impedance match, demonstrated by lack of signal ringing event in the fastest measurements (Fig. 3), in parallel with stability that is extended beyond the minute time domain (Fig. 2c). Furthermore, since there is no need to apply a voltage strobe to the probe-light source, practically, there are no limitations on the length of the data acquisition times. On the fast end, however, the limits for kinetic measurements are imposed by the duration of the laser excitation pulse.

## ACKNOWLEDGMENTS

We acknowledge with thanks the support of the Photonics Center at Boston University and the US Department of Energy, Office for Basic Energy Science. We also extend our gratitude to Professors R. W. Redmond and W.G. McGimpsey and to Mr. E. Hazen for helpful discussions.

## REFERENCES

1. Jones, G., II and V.I. Vullev, 2002. Photoinduced electron transfer between non-native donor-acceptor moieties incorporated in synthetic polypeptide aggregates. Organic Lett., 4: 4001-4004.

2. Vullev, V.I. and G. Jones, 2002. Photoinduced electron transfer in alkanoylpyrene aggregates in conjugated polypeptides. Tetrahedron Lett., 43: 8611-8615.
3. Jones, G., II and V.I. Vullev, 2002. Medium effects on the photophysical properties of terbium(iii) complexes with pyridine-2, 6-dicarboxylate. Photochemical. Photobiol. Sci., 1: 925-933.
4. Jones, G., II and V.I. Vullev, 2002. Medium effects on the stability of terbium(iii) complexes with pyridine-2, 6-dicarboxylate. J. Phys. Chem. A, 106: 8213-8222.
5. Luedemann, H.-C., F. Hillenkamp and R.W. Redmond, 2000. Photoinduced hydrogen atom transfer in salicylic acid derivatives used as matrix-assisted laser desorption/ionization (maldi) matrixes. J. Phys. Chem. A, 104: 3884-3893.
6. Krieg, M., M.B. Srichai and R.W. Redmond, 1993. Photophysical properties of 3, 3'-dialkylthiacarbocyanine dyes in organized media: Unilamellar liposomes and thin polymer films. Biochimica et Biophysica Acta, 1151: 168-174.
7. Janata, E., 1992. Instrumentation of kinetic spectroscopy. 10. A modular data acquisition system for laser flash photolysis and pulse radiolysis experiments. Rad. Phys. Chem., 40: 437-443.
8. Patterson, L.K. and J. Lilie, 1974. Computer-controlled pulse radiolysis system. Intl. J. Rad. Phys. Chem., 6: 129-141.
9. Malba, V., G. Jones, II and E.D. Poliakoff, 1985. Interfacing for laser flash photolysis experiments: A new approach. Photochem. Photobiol., 42: 451-455.
10. Fenster, A., J.C. LeBlanc, W.B. Taylor and H.E. Johns, 1973. Linearity and fatigue in photomultipliers. Rev. Scientific Instruments, 44: 689-694.
11. Kyushima, H., Y. Hasegawa, A. Atsumi, K. Nagura, H. Yokota, M. Ito, J. Takeuchi, K. Oba, H. Matsuura and S. Suzuki, 1994. Photomultiplier tube of new dynode configuration. IEEE Trans. Nucl. Sci., 41: 725-729.
12. Kerns, C. R., 1977. High-rate phototube base. IEEE Trans. Nucl. Sci., 24: 353-355.
13. Horowitz, P. and W. Hill, 1989. Precision Circuits and Low-noise Techniques. In: The Art of Electronic. 2nd Edn., Cambridge University Press, UK.
14. Keene, J.P. and C. Bell, 1973. Automatic circuits for backing off photodetector signal in kinetic spectrophotometry. Intl. J. Rad. Phys. Chem., 5: 463-477.
15. Janata, E., 1986. Base-line compensation circuit for measurement of transient signals. Rev. Scientific Instruments, 57: 273-275.
16. Alfano, R.R. and N. Ockman, 1968. Methods for detecting weak light signals. J. Optical Soc. America, 58: 90-95.
17. Robben, F., 1971. Noise in measurement of light with photomultipliers. Appl. Optics, 10: 776.
18. Foord, R., R. Jones, C.J. Oliver and E.R. Pike, 1969. Use of photomultiplier tubes for photon counting. Appl. Optics, 8: 1975.
19. Janata, E., 1992. Instrumentation of kinetic spectroscopy. 8. The use of baseline compensation in the subnanosecond time domain. Rad. Phys. Chem., 39: 319-320.
20. Johnson, J.B., 1928. Thermal agitation of electricity in conductors. Phys. Rev., 32: 97-109.
21. Jones, G., Z.M. Feng and C. Oh, 1995. Photoinduced electron-transfer for an eosin tyrosine conjugate-activity of the tyrosinate anion in long-range electron-transfer in a protein-like polymer matrix. J. Phys. Chem., 99: 3883-3888.
22. Wintgens, V., J.C. Scaiano, S.M. Linden and D.C. Neckers, 1989. Transient phenomena in the laser flash-photolysis of rose-bengal c-2' ethyl-ester c-6 sodium-salt. J. Org. Chem., 54: 5242-5246.
23. Lamture, J.B., Z.H. Zhou, A.S. Kumar and T.G. Wensel, 1995. Luminescence properties of terbium(iii) complexes with 4-substituted dipicolinic acid analogs. Inorg. Chem., 34: 864-869.
24. Hemmila, I., 1985. Time-resolved fluorometric-determination of terbium in aqueous-solution. Anal. Chem., 57: 1676-1681.